

# Fracture toughness of a high-strength beryllium at room temperature and 300° C

M. W. PERRA\*, I. FINNIE

*Department of Mechanical Engineering, University of California, Berkeley, California, USA*

The fracture toughness of a high yield strength grade of hot-pressed beryllium block was determined at room temperature and 300° C. Fatigue cracks were generated in double-cantilever beam specimens by a reversed loading method. Room temperature fracture toughness values from specimens with electric discharge machined notches fell within the scatter band of values from specimens with fatigued precracks. Load-displacement records generated from test on specimens with machined notches exhibited the expected linearity. However, the records were nonlinear from tests on specimens with long cracks formed by repeated propagation and arrest. Evidence points to a crack-closure phenomenon rather than plasticity as the source of the nonlinearity. The fracture toughness data show that specimen orientation or test temperature have little effect. By contrast, reported ductility values for this material are very sensitive to both these variables. The mean value of the fracture toughness ranged from 9.0 MPa m<sup>1/2</sup> (8.1 ksi in.<sup>1/2</sup>) at 23° C to 10.8 MPa m<sup>1/2</sup> (9.7 ksi in.<sup>1/2</sup>) at 300° C. These values are among the lowest ever reported for beryllium.

## 1. Introduction

Beryllium is an attractive material for many applications. However, its use as a structural material is limited by its tendency to brittle fracture at low stress intensities. At room temperature, tensile elongations of less than 3% are commonly reported for hot-pressed beryllium; no shear lips are evident on fracture surfaces and cleavage mechanisms dominate. The propensity of beryllium to brittle fracture presumably arises from its ease of cleavage on several planes (most conspicuously the basal plane) and the resistance of its lattice to the generation and motion of dislocations having a component resolvable along the *c*-axis.

The influence of elevated temperature on the resistance of beryllium to fracture is largely undetermined, although this is a problem of considerable practical significance. Such information would be of value, for instance, in a program for controlling the fracture of welded parts.

Only a small amount of data is available in the literature on the elevated-temperature fracture

toughness of beryllium. The results of Harrod *et al.* [1] for S-200 grade beryllium indicate that between 23 and 260° C the fracture toughness increases from about 20 MPa m<sup>1/2</sup> (18 ksi in.<sup>1/2</sup>) to 38 MPa m<sup>1/2</sup> (34 ksi in.<sup>1/2</sup>). The value for 260° C was based on the results of a single test. More recently, the data of Shabbits and Longsdon [2] on S-200 grade beryllium indicated no appreciable increase in toughness between 23 and 150° C, but showed a rapid increase in toughness between 105 and 260° C going from about 10 MPa m<sup>1/2</sup> (9 ksi in.<sup>1/2</sup>) to about 16 MPa m<sup>1/2</sup> (14 ksi in.<sup>1/2</sup>), respectively. These values were obtained from fatigue-precracked compact-tension specimens oriented with the crack plane perpendicular to the pressing direction, and were based on the results of three tests at 150° C and two sets at 260° C. In this temperature range, no data were generated from specimens oriented with the crack plane parallel to the pressing direction.

The present study has been undertaken with the objective of determining the temperature de-

\* Present address: Sandia Laboratories Livermore, Livermore, Ca94550, USA

pendence of the fracture toughness of a high yield strength beryllium at room temperature and 300° C.

## 2. Material and test specimens

The beryllium used in this study was a vacuum-hot pressed block of high-yield material. The chemistry was within the limits of S-200 grade, but a deliberate attempt was made to produce a high yield strength. Some chemical, physical, and mechanical properties of this material are listed in Table I and II. In comparison with most commer-

TABLE I Chemical composition of high yield grade beryllium

	According to supplier	According to Battelle Columbus Laboratory	
	(ppm)	Chemical determination (ppm)	Determination by neutron-activation analysis (ppm)
BeO	20040	—	14 100
Fe	1680	1500	—
C	1230	1430	—
Al	620	400	469
Mg	80	60	—
Si	470	200	—

TABLE II Tensile properties ( $\dot{\epsilon} = 6.4 \times 10^{-4} \text{ sec}^{-1}$ ) of high yield grade beryllium at room temperature.

Property [3]	Value
0.2% offset yield strength (MPa)	338
Ultimate strength (MPa)	386
Total elongation (%)	2.1
Reduction of area (%)	2.6
Density (% of theoretical)	99.45 to 99.71
Grain size ( $\mu\text{m}$ )	$8.8 \pm 0.03$

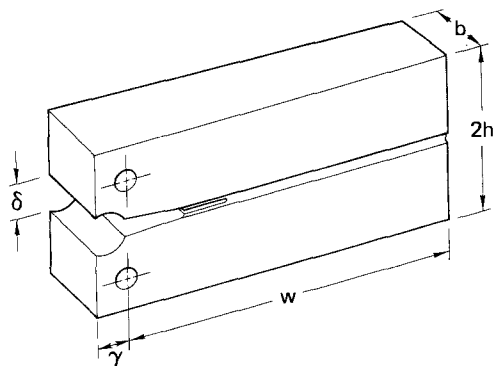


Figure 1 Double cantilever-beam specimens having dimensions (in mm)  $2h = 19.1$ ,  $b = 8.92$ ,  $w = 47.22$ ,  $\gamma = 3.58$ . Electric discharge machined slot is 1.27 mm long and 0.102 mm thick. Side grooves each have depth of 0.610 mm and a root radius of 0.051 mm.

cial grades of beryllium, this material has a rather low density, small grain size, and high iron content. The specimens were cut from the block in two crack-plane orientations with respect to the pressing direction. There were 15 transverse specimens (i.e., crack-plane parallel to the pressing direction) and 10 longitudinal specimens (i.e., crack-plane perpendicular to the pressing direction). The double-cantilever beam (DCB) specimens used in this study are shown in Fig. 1.

## 3. Fatigue Precracking

Some specimens were tested with the notch in the electric discharge machined condition, but most frequently, fatigue cracks were grown beyond the tip of the notch. Controlled growth of fatigue cracks using reversed loading which has been reported by Jones *et al.* [4] and others [2, 5], was used in the present work. Fatigue cracks were produced with the ratio of maximum-to-minimum applied load equal to  $-1$ . A controlled displacement testing mode was used at a frequency of load reversal of 20 Hz. Unwanted displacements in the rigid load train were minimized by using tight-fitting loading pins and pretorqued connections. Because no universal joints were used, care was taken in alignment to minimize eccentric loading on the specimens. The alignment of the loading grips allowed the loading pins a deviation from parallel of no more than  $0.08^\circ$ . With a maximum load corresponding to a fatigue stress intensity factor  $K_f$  of  $6.5 \text{ MPa m}^{1/2}$  ( $5.9 \text{ ksi in.}^{1/2}$ ), fatigue cracks were observed to initiate and grow to approximately 1.3 mm in length in  $8 \times 10^4$  cycles. At slightly smaller stress intensities, for example  $5.6 \text{ MPa m}^{1/2}$  ( $5 \text{ ksi in.}^{1/2}$ ), no crack was observable after a similar number of cycles. Difficulty was encountered in propagating fatigue cracks in a controlled manner at the stress intensities employed, and erratic growth rates were frequently observed. It was found from later test results that the ASTM requirement of  $K_f < 0.6K_{IC}$  was not satisfied.

## 4. Test procedure and load-displacement results

Specimens were pulled to fracture at a crosshead speed of  $1.12 \times 10^{-3} \text{ mm sec}^{-1}$ . Those for the high temperature tests were heated in an argon atmosphere. The change of specimen temperature during a test did not exceed  $2^\circ \text{ C}$ . The clip gauge used for measuring the displacement  $\delta$  was made of a type 416 ferritic stainless steel, and a strain-gauge

adhesive which remained stable at temperatures up to 310°C was used. The clip gauge was calibrated at high temperatures (150 and 300°C) by means of a specially designed apparatus consisting of concentric quartz tubes inside the furnace and a micrometer outside.

Specimen compliance was obtained as a function of "crack" length by extending the 0.102 mm slot by electric discharge machining. Because opening displacements were measured at the end of the specimen rather than under the point of loading, a correction factor was applied to the apparent compliance to determine the actual specimen compliance. The correction, which is obtained from simple beam theory and the results of Mostovoy *et al.* [6] is

$$C_{\text{actual}} = C_{\text{apparent}} - \frac{6\gamma}{Ebh} \left[ (1 + \nu) + 2 \left( \frac{a + 0.6h}{h} \right)^2 \right]$$

where  $\gamma$  is the perpendicular distance from the centre of the loading pins to the knife edges at the end of the specimen,  $E$  is Young's modulus,  $\nu$  is Poisson's ratio,  $a$  the crack length, and  $b$  and  $h$  are the cantilever thickness and height, respectively. Fig. 2 is a plot of the observed compliance (corrected for the location of displacement measurement) versus machined crack length. Also plotted is the approximate analytic expression determined by Mostovoy *et al.* [6],

$$C = \frac{8}{Ebh^3} \left[ (a + 0.6h)^3 + \frac{3(1 + \nu)ah^2}{4} \right]$$

It is seen that the experimental and the analytical results agree very well. The compliance calibration

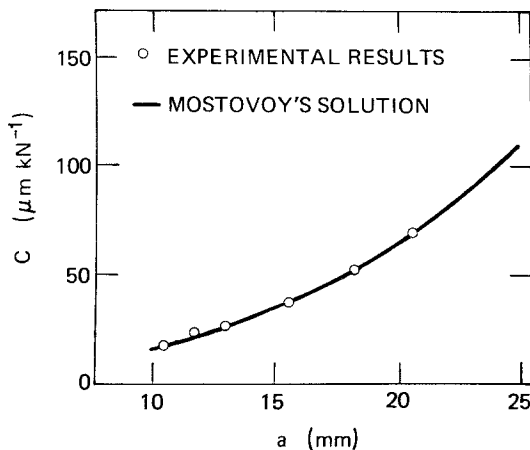


Figure 2 Experimentally determined compliance calibration, compared with solution of Mostovoy *et al.* [6].

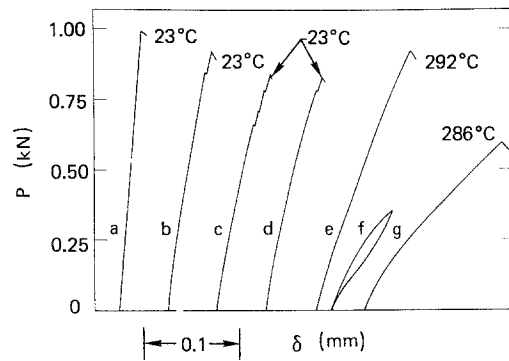


Figure 3 Load displacement record for a transverse specimen. Crack lengths (in mm) (a) 13, (b) 20, (c) 20, (d) 23, (e) 24, (f and g) 34.

at 300°C also agrees well with these results, indicating that between 23 and 300°C compliance is not a function of temperature. The load-displacement results for these compliance tests were linear from small loads up to loads as large as those used for crack propagation in a fracture-toughness test. Within the sensitivity of the clip gauge, displacement was completely reversible after unloading the specimen.

For specimens with natural cracks (i.e. cracks formed by repeated propagation and arrest) however, the load-displacement record linearity depended strongly on the length of the crack. For cracks which extended only short distances ( $\leq 1.5$  mm) beyond the tip of the machined slot, the record was essentially linear up to the point of fracture, and satisfied ASTM linearity requirements. Nonlinearity became more pronounced for longer cracks. An example of this behaviour is given in Fig. 3. For long crack-lengths, the curvature of the record decreases with increasing loads; linearity is most closely approximated at higher loads.

As shown in Fig. 3 (curve *f*) if a subcritical load (that is, a load which was less than that required to extend the crack) was applied to a specimen with a long natural crack, and if the specimen was subsequently unloaded, the unloading curve did not coincide with the loading curve. This curve also indicates no appreciable residual displacement after a complete loading-unloading cycle.

Because the nonlinearity shown in Fig. 3 was never observed with machined cracks tested under identical conditions, the nonlinearity cannot reasonably be attributed to errors in the measurements of loads or displacements. Faulty seating of the clip gauge or the loading pins must be ruled

out as possible sources for this effect. Further, because the nonlinearity decreased with increasing loads and because there were no observable residual displacements on unloading from subcritical loads, crack-tip plasticity and plastic flow in the vicinity of the loading pins must also be ruled out.

The nonlinearity manifested itself as increasing specimen compliance with increasing load. This phenomenon has been observed by Jones, Bubsey and Brown [4] in beryllium bend specimens subjected to fatigue pre-cracking. These authors suggested that the nonlinearity was associated with the crack-closure phenomenon described by Elber [7]. Elber has defined a crack as being closed when the compliance of the body is the same as the compliance of an identical but uncracked body under the same load system. Assume for the moment that a crack of length  $a$  in an unloaded elastic body is closed due to internal forces which exist in the body. Then, as loads are applied which overcome the closing forces and gradually open the crack, the compliance will also gradually increase from that of an uncracked body to that of a body with an open crack of length  $a$ .

If we postulate the existence of crack-closing forces, we can explain the dependence of compliance on applied load as exhibited by these specimens. The crack may be considered to consist of both open and closed parts; that is, as shown in Fig. 4a,

$$a = a_0 + a_c.$$

As a result of the postulated closing forces,  $a_0$  increases monotonically with  $P$  and the compliance smoothly increases with  $P$ , as shown in Fig. 4b. It

is apparent that the nonlinearity would be marked for DCB specimens with long cracks ( $a$  being several times larger than  $a_i$ ).

The influence of crack closure on compliance in the DCB specimen was demonstrated by the following technique: a 0.102 mm slot was machined by electric discharge in a specimen to simulate a long ( $a = 30$  mm), open crack. A tensile load of 267 N was applied to the specimen. This would correspond to a stress intensity of  $4.4 \text{ MPa m}^{1/2}$  ( $4 \text{ ksi in.}^{1/2}$ ) if it were applied to a specimen with a natural crack of the same length. The load-displacement record was linear. Shimstock slightly thicker than the slot was then placed between the separated arms of the specimen, with the stock wedged as close to the notch tip as interference would allow. Subsequent load-displacement records showed a strong nonlinearity similar to that of Fig. 4b.

Measurements of opening displacements near the tip of a long (about 20 mm) natural crack were made as a function of applied load. The reference points for displacement measurement were attached rigidly to both arms of the DCB specimen at a small distance (about 2.5 mm) behind the crack tip. The signal from the high-sensitivity displacement transducer was displayed directly on a digital voltmeter. The resulting plot of load versus displacement (Fig. 5) indicates that substantial loads had to be applied before any resolvable opening occurred. These data are consistent with the hypothesis that a crack-closing phenomenon played a role in the observed nonlinearities.

The source of the postulated crack-closing

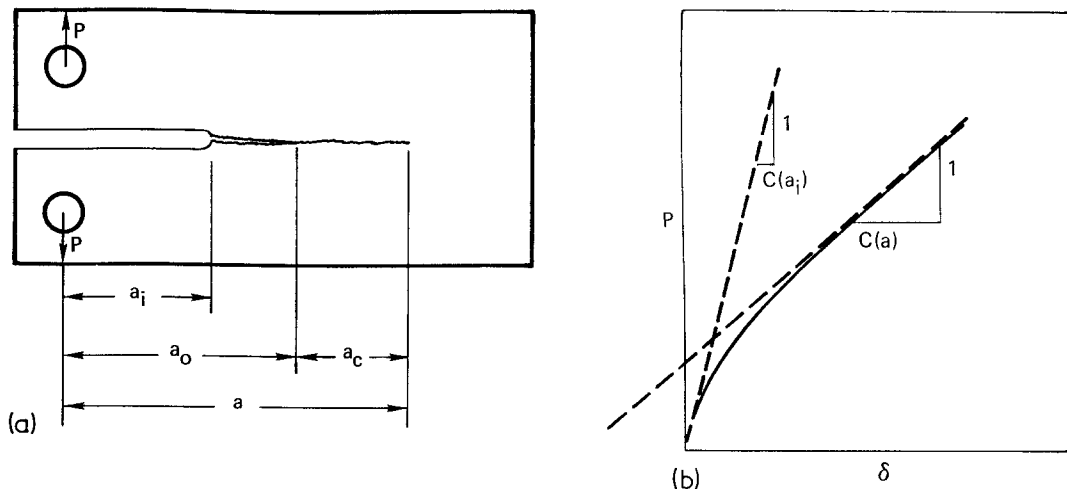


Figure 4 The influence of gradual crack opening on the compliance of a DCB specimen.

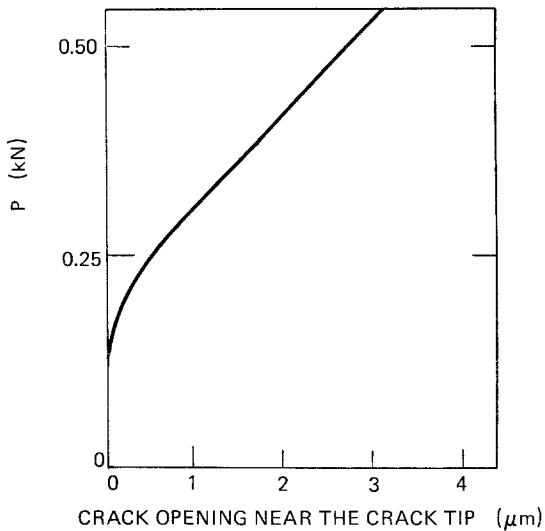


Figure 5 Load as a function of crack opening near the tip of a long crack formed by repeated crack initiation and arrest.

forces in a naturally cracked specimen remains to be identified. It is likely that the crack faces do not fit perfectly after unloading because of plastic deformation and secondary cracking left in the wake of the main crack. As the applied load was removed, the putative lack of fit would prevent the arms of the specimen from returning to their original position with respect to one another. Consequently, a residual compressive force would be transmitted across the points of contact of the crack faces. In this manner, crack-face interference could generate internal forces leading to nonlinearities of the load–displacement record.

In these experiments, microcracking frequently occurred, showing up as small steps in the load–displacement record. (See, for example, Fig. 3, curve c). These events were detected by an acoustic transducer. No optically observable increase in crack length was produced by microcracking. As pointed out by Jones *et al.* [4], microcracking is to be expected in beryllium in the light of its very low basal-plane fracture propagation energy.

### 5. Crack length determination

After fatigue precracking or fracture-toughness testing, crack-length measurements were made on both sides of the specimen, using an optical microscope at 100× magnification. Because optical techniques of crack-length determination frequently gave results which were not reproducible, other techniques were utilized, including ultra-

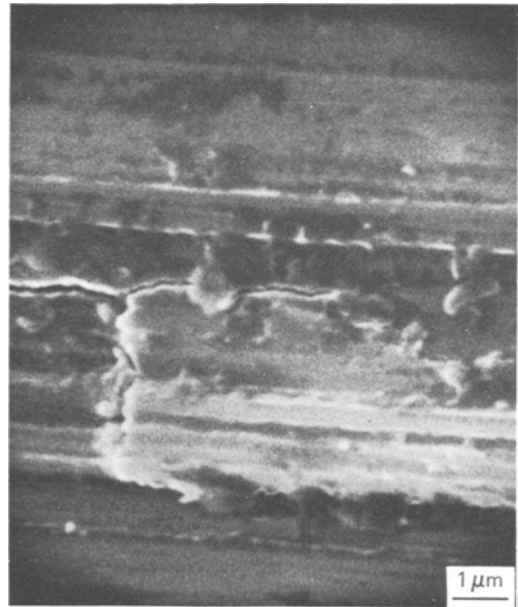


Figure 6 Scanning electron micrograph of a fatigue crack in the root of a side groove.

sonic, radiographic, and dye-penetrant methods. However, none of these techniques was entirely satisfactory.

The scanning electron microscope was also used and revealed cracks which would not be visible in an optical microscope. One can infer from Fig. 6, which is a scanning electron micrograph of a crack in the root of a side groove, that optical measurements of crack length are likely to be biased toward short values. Unfortunately it is not practical to use the scanning microscope as a routine method for crack length measurement.

An indirect method of crack length measurement involved comparing the experimentally determined compliance (defined as the inverse of the slope of the linear portion of the load–deflection record) with the standard plot of compliance versus crack length. For the cases in which the nonlinearity persisted to the critical load, the maximum compliance was used. If crack closure was the dominant source of the nonlinearity, then the use of maximum compliance is valid. The correlation between the longest of the two optically determined crack lengths (obtained from the two sides of the specimen), and the crack length as determined from the observed compliance, was superior to the correlation between the average of the optical measurements and the compliance–crack length. This is demonstrated in Fig. 7. The superior

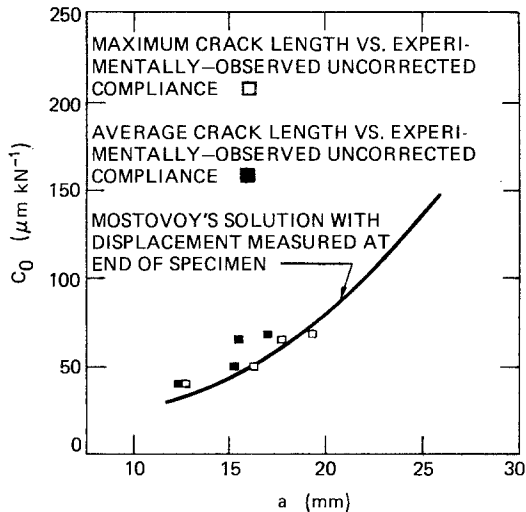


Figure 7 Comparison of experimental crack length and compliance values with solution of Mostovoy *et al.* [6].

correlation in Fig. 7 with maximum observed crack length was taken to be evidence that optically determined measurements were biased toward short values.

### 6. Numerical values of fracture toughness

After establishing the compliance of the specimen as a function of crack length, the energy-release rate  $\mathcal{G}$  and the plane strain stress intensity factor  $K_I$  were computed using through the standard relations:

$$\mathcal{G} = \frac{P^2}{2b_N} \left( \frac{dc}{da} \right); \quad K_I = \left[ \frac{\mathcal{G} E}{1 - \nu^2} \right]^{1/2}$$

where  $P$  is the applied load and  $b_N$  the specimen thickness between side grooves. It was not possible to compute  $K_{IC}$  values from the recorded data because of the nonlinearity of the load–displacement records. Maximum loads were used to compute the critical stress intensity factors, which are reported as  $K_{max}$  rather than  $K_{IC}$ . As mentioned previously, the maximum load did not always correspond to the initiation of detectable cracking during a test. If acoustic-emission techniques had been employed in the determination of load for the calculation of fracture toughness, significantly smaller values of fracture toughness would have been derived. As discussed above, specimen compliance was used as an independent check on crack length. Occasionally, the discrepancy between the length of the crack as determined optically and the length determined from specimen compliance exceeded 2.5 mm. When this occurred, the uncertainty in crack

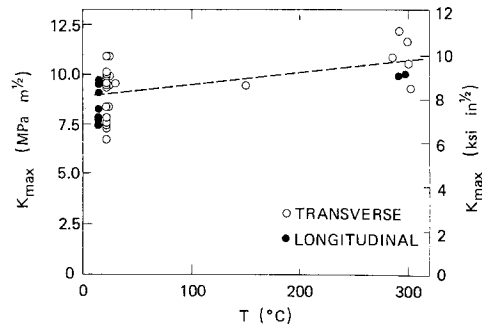


Figure 8  $K_{max}$  as a function of temperature.

length was considered to be unacceptable and the data from that test were ruled to be inadmissible. Values of  $K_{max}$  versus temperature for both transverse and longitudinal specimens are plotted in Fig. 8.

No significant differences are observed for  $K_{max}$  between the transverse and longitudinal orientations. The fracture-toughness values may increase slightly with increasing temperature but the data are inconclusive in view of the scatter. The toughness values for room temperature tests range from 6.8 to 11.0  $\text{MPa m}^{1/2}$  (6.1 to 9.9  $\text{ksi in}^{1/2}$ ). The average of 24 room temperature tests is 9.0  $\text{MPa m}^{1/2}$  (8.1  $\text{ksi in}^{1/2}$ ).

No significant temperature dependence of yield strength or of ultimate strength was observed for temperatures between 20 and 300°C for this material [3]. Over this same temperature range, the reduction in area of longitudinal specimens fell from approximately three percent to less than one percent, whereas the reduction in area of transverse specimens increased from approximately 4 to 30% [3].

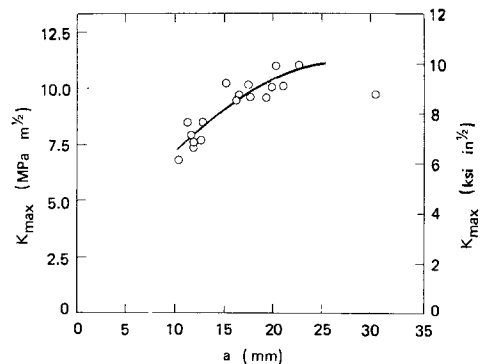


Figure 9  $K_{max}$  as a function of crack length for transverse specimen at 23°C.

Fig. 9 is a plot of  $K_{\max}$  versus crack length for the transverse specimens at 23° C. Our measurements showed an increase in  $K_{\max}$  with crack length for 10 mm <  $a$  < 15 mm. A similar trend has been observed in testing limestone [8]. It appears unlikely that the variation of  $K_{\max}$  with  $a$  is due to experimental error; a more likely explanation is the value of the stress intensity factor  $K$  at fracture is influenced by the non-singular terms in the series expansion for stresses near the tip of a crack. It has been suggested by Finnie and Saith [9] that the second term in the series expansion has an influence on the directional stability of cracks. Larsson and Carlsson [10] have demonstrated that for the same  $K$  values, different types of specimens will have varying sizes of plastic zones in the case of small-scale yielding at the crack tip. Rice [11] has shown that in the series expansion the magnitude of the second term relative to the first, or singularity term, is responsible for this effect. There is at this stage little clear-cut experimental evidence to show the influence of subsequent terms in the series expansion on fracture-toughness. However in the double-cantilever-beam test, the value of the second series expansion term, relative to  $K$ , increases rapidly as crack length increases. It is also conceivable that the residual stresses responsible for crack closure in specimens with longer cracks have an influence on the measured fracture-toughness. These aspects of the double cantilever-beam specimen deserve further attention.

That the distribution of points in Fig. 8 may not be a true indication of scatter can be seen in Fig. 9. For any given crack length in Fig. 9, the extreme values do not differ by more than 2.2 MPa m<sup>1/2</sup> (2 ksi in.<sup>1/2</sup>). Returning to Fig. 8, in which crack length is an implicit variable, we note that the extreme values for the same set of data differ by 4.4 MPa m<sup>1/2</sup> (4 ksi in.<sup>1/2</sup>).

Several tests were performed at room temperature to determine the difference between fracture toughness of specimens in the fatigue-precracked and in the machined conditions. No significant influence of notch-root preparation on  $K_{\max}$  could be detected.

## 7. Fractography

An examination of fatigue and fast-fracture surfaces was made using a scanning electron microscope. In Fig. 10 a fatigue area shows isolated regions in which cleavage planes make large angles

with respect to each other. The adjacent areas of the fatigue surface appear to be highly textured and rough, as can be seen in Fig. 11. There is apparently some debris on the fatigue surface. It is possible that the peculiar appearance of these fatigue surfaces could, in large part, result from damage accumulated during the reversed loading procedure.

A fast-fracture region of a specimen tested at 302° C is shown in Fig. 12. This fractograph reveals predominantly flat transgranular cleavage. There were no apparent differences between room temperature and elevated temperature fast-fracture surface.

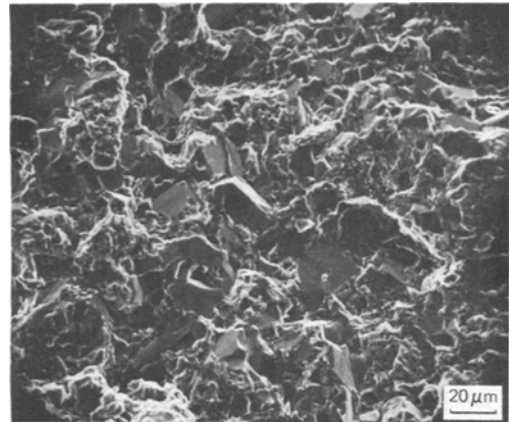


Figure 10 Scanning electron micrograph of a fatigued region.

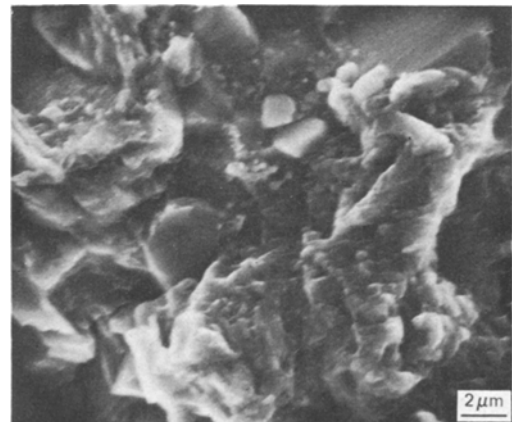


Figure 11 Scanning electron micrograph of a fatigued region.

## 8. Conclusions

From the results of this study, the following conclusions can be drawn:

(1) Using reversed-loading procedures, fatigue cracks 1.27 mm in length were grown (typically, in

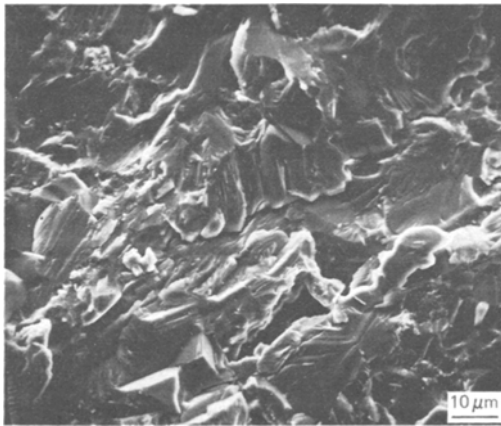


Figure 12 Scanning electron micrograph of a fast fracture region at 302°C.

$8 \times 10^4$  cycles) at a fatigue stress intensity of 6.5 MPa m<sup>1/2</sup> (5.9 ksi in.<sup>1/2</sup>). Cracks would not initiate or grow at lower stress intensities. Uncertainty as to the extent of plasticity and twinning in the vicinity of the crack tip may limit the usefulness of this technique in standard fracture toughness testing.

(2) The values of  $K_{max}$  obtained from specimens with machined notches did not differ significantly from those obtained from fatigue-precracked specimens.

(3) Specimens with long cracks exhibited increasing compliance as applied loads increased. This was identified as a crack closure phenomenon. While often observed in cracks propagated by fatigue, such behaviour has not, to our knowledge, been observed before for cracks formed by repeated propagation and arrest. For short cracks, the load-displacement records satisfied ASTM requirements for linearity.

(4) The fracture toughness of this material is only a weakly increasing function of temperature. At 23°C the mean value of toughness from 24 tests is 9.0 MPa m<sup>1/2</sup> (8.1 ksi in.<sup>1/2</sup>) with a lower extreme of 6.8 MPa m<sup>1/2</sup> (6.1 ksi in.<sup>1/2</sup>). At 300°C the mean value of toughness from 7 tests is 10.8 MPa m<sup>1/2</sup> (9.7 ksi in.<sup>1/2</sup>) with a lower extreme of 9.7 MPa m<sup>1/2</sup> (8.5 ksi in.<sup>1/2</sup>). The room temperature values are among the lowest ever reported for beryllium. In contrast to our fracture toughness measurements, ductility of this material has been reported [3] to be strongly influenced by speci-

men orientation at elevated temperature. These results suggest that fracture toughness is not related to reduction of area in the tension test when cleavage mechanisms dominate.

(5) Subcritical crack growth (microcracking) occurred at stress intensities as low as 60% of the critical stress intensity.

(6) There is no appreciable orientation effect for this material. At room temperature, the mean value of toughness from 18 tests of transverse specimens is 9.1 MPa m<sup>1/2</sup> (8.2 ksi in.<sup>1/2</sup>) whereas the mean value of toughness from 7 tests of longitudinal specimens is 8.6 MPa m<sup>1/2</sup> (7.8 ksi in.<sup>1/2</sup>).

### Acknowledgements

This work was carried out at the Lawrence Livermore Laboratory of the University of California. The advice and guidance of James R. Hauber and Haskell Weiss throughout the course of this work, as well as the skillful assistance of Bernard A. Kuhn in testing, made the project possible. Their contributions were indispensable and are gratefully acknowledged.

### References

1. D. L. HARROD, T. F. HENGSTENBERG and M. J. MANJOINE, *J. Mater.* **4** (1969) 618.
2. W. O. SHABBITS and W. A. LOGSDON, *J. Test. Eval.* **1** (1973) 110.
3. S. H. GELLES, Summary Report on Characteristics of Commercial Vacuum-Hot-Pressed Beryllium. Part II, Lawrence Livermore Lab., Rept. UCRL-13589 (1972).
4. M. H. JONES, R. T. BUBSEY and W. F. BROWN Jr., *J. Test. Eval.* **1** (1973) 100.
5. H. CONRAD, J. HURD and D. WOODARD, *ibid* **1** (1973) 88.
6. S. MOSTOVOY, P. B. CROSLY and E. J. RIPLING, *J. Mater.* **2** (1967) 66.
7. W. ELBER, *Engr. Fract. Mech.* **2** (1970) 37.
8. R. A. SCHMIDT, *Experimental Mechanics*, **16** (1976) 161.
9. I. FINNIE and A. SAITH, *Int. J. Fract.* **9** (1973) 484.
10. S. G. LARSSON and A. J. CARLSSON, *J. Mech. Phys. Sol.* **21** (1973) 263.
11. J. RICE, *ibid* **22** (1974) 17.

Received 20 December 1976 and accepted 8 February 1977.